11th World Congress on Computational Mechanics (WCCM XI)
5th European Conference on Computational Mechanics (ECCM V)
6th European Conference on Computational Fluid Dynamics (ECFD VI)
E. Oñate, J. Oliver and A. Huerta (Eds)

Analysis on the plastic dynamic response of the reinforced concrete rectangular plate under explosive loading

Jian He[1], Kongming Wu[2]

[1]Aerospace and civil Engineering Department
Harbin Engineering University
No,145 NanTong Street, 150001, Harbin, China
Email:Hejian@hrbeu.edu.cn

[2]Aerospace and civil Engineering Department
Harbin Engineering University
No,145 NanTong Street, 150001, Harbin, China
Email:WKM137846020@126.com

Key words: *Reinforced concrete rectangular plate, Rigid-plastic, Membrane force effect, Numerical analysis*

Abstract: To analyze the failure mode and final deformation of concrete rectangular plate under explosive loading, the energy method and plastic hinge theory is employed by regarding concrete as perfect rigid-plastic material. Large plastic deformation is usually brought about by explosion applied to the plate, while it is constrained by supporting boundary from which compressive reaction would effect on the plate when large deformation takes place. By assuming that the compressive reaction is acted on the equilibrium surface, a reaction parameter is defined in the motion balance equations of small deformation to take the advantages of supports into account for large deformation. There are two different failure modes of plate under different explosive peak overpressures, so the motion balance equations during and after the action of explosive loading are deduced in accordance with small or large deformation, which contributes to the failure process and final deformation of plate by employing moving hinges theory. In order to verify the theoretical method, numerical simulations of reinforced concrete plate under explosion are carried out to investigate on how the explosive charge impacts on its failure modes. By comparing the numerical results and theoretical ones, the analysis method in this paper is proved effective and available to analyze the plastic deformation and failure modes of reinforced concrete rectangular plate under explosion.

1 INTRODUCTION

Usually, Limit Analysis Method or Classical Yield Theory is often employed to research on the deformation and failure of reinforced concrete plate acted on static loads. Subjected

to dynamic loads, the plastic behavior of reinforced concrete slab comes up ahead of that under static loads. So the perfectly rigid-plastic model is proposed to analyze the deformation of reinforced concrete plate under explosive loads.

In order to simplify the calculation, the blast load is assumed as triangular load with rising period [1]:

$$p(t)=\begin{cases} p_m t/t_m, & 0\le t\le t_m \\ p_m\left(t-t_s\right)/(t_m-t_s), & t_m\le t\le t_s \end{cases} \tag{1}$$

in which t_m is the moment when peak load pressure comes up, p_m is the peak pressure.

2 THE BASIC EQUARIONS OF PLATE

The reinforced concrete material is idealized as completely uniform, continuity, isotropic rigid-plastic material, and the size change of the specimen with deformation is ignored. When determining the motion and geometric equilibrium equations, the theory considering no strain rate, static yield condition and plastic flow rule are employed. If the thickness of plate is h, the uniaxial tensile yield stress is Y, then the plastic ultimate moment on per unit plate is $M_0=\sigma_0 h^2/4$. When Tresca yield criterion applied, there is $\sigma_0=Y$; Mises yield criterion applied, $\sigma_0=2Y/\sqrt{3}$.

Yield line theory, namely broken line theory, is established by extending plastic hinge theory of beam to shell structures, while plastic hinge of shell structures shows as a narrow plasticity zone along one direction [2]. There are some assumptions of yield line to structure its shape: the yield line is produced firstly where ultimate bending moment comes into being; along with the line only the effect of moment is accounted in while the torque and shear are ignored; no elastic deformation of rigidity pieces between yield lines is considered; and viscous damping are ignored[3].

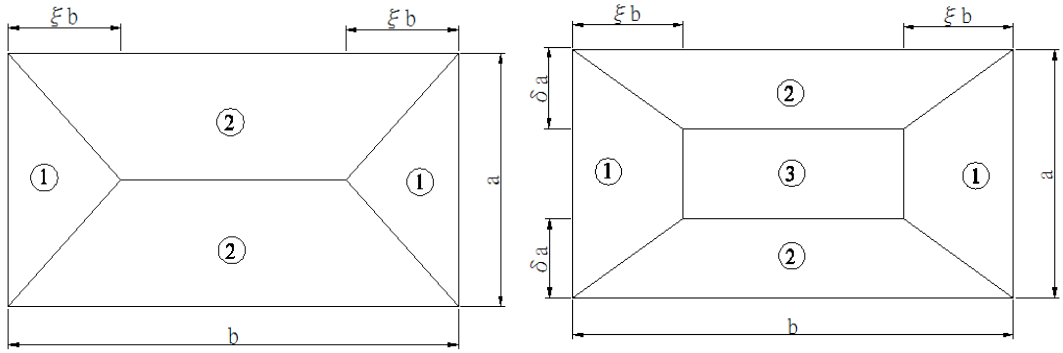

a. *Failure mode A* *b. Failure mode B*

Fig.1 Two patterns of the failure mode

Based on the assumptions and experiments, the ultimate states of rectangular rigid-plastic plate under uniform load $p(t)$, namely the plastic failure modes with two possible patterns [4]are as shown in Fig.1.

According to the principle of maximum consume energy, all the power of external force is consumed by the yield lines, then corresponding limit equilibrium equations are:

$$\begin{aligned} &p_0(3-4\delta_p)\xi_p^2 = 6\alpha \\ &p_0(3-4\xi_p)\delta_p^2 = 6\gamma^2\alpha \end{aligned} \quad \text{(A)} \qquad \begin{aligned} &p_0\xi_p^2 = 6\alpha \\ &p_0(3-4\delta_p) = 6\gamma^2\alpha \end{aligned} \quad \text{(B)} \qquad (2)$$

in which α is boundary supporting parameter, and $\alpha = 1$ means simply supporting, $\alpha = 2$ clamped supporting; ξ_p, δ_p are dimensionless parameter of rigid area at plastic limit states($0 \le \xi_p \le 1/2, 0 \le \delta_p \le 1/2$); γ is length-width ratio ($\gamma = b/a \ge 1$); $p_0 = P_0 b^2 / M_0$, in which p_0 is plastic limit load.

3 MEMBRANE FORCE EFFECT

Large deformation of shell structure comes up when impact load applied, and tensile and flexural capacity of plate will be strengthened by the reaction force of supports. The effect is similar to the tension increased by large deformation of thin film, so it's called membrane force effect.

Under the united action of bending moment and membrane force, the rate of plastic power consumed by unit length of yield line is[5]:

$$\dot{D}_i = (N\omega - M)\dot{\theta}_i \tag{3}$$

where ω is deflection of yield line; N and M are membrane force and bending moment respectively; $\dot{\theta}_i$ is relative rotation angle between both sides of yield line.

Yield criterion of maximum normal stress with effect of both bending moment and membrane force accounted in is:

$$\left|M / M_0\right| + \left(N / N_0\right)^2 = 1 \tag{4}$$

in which M_0, N_0 are plastic ultimate moment and tensile stress respectively. The nonlinear function of yield surface is too complicated to employ, so the yield condition is simplified as two separate conditions:

$$\left|M / M_p\right| = 1, \qquad \left|N / N_p\right| = 1 \tag{5}$$

Based on associated flow rule and Drucker postulate, the dissipation function of yield lines of the plate can be obtained[6]:

$$\dot{D}_i = \begin{cases} M_0\left(1+3\omega^2/H^2\right)\dot{\theta}_i & \omega/H \le 1 \\ 4M_0\omega/H\dot{\theta}_i & \omega/H > 1 \end{cases} \tag{6}$$

So the total power consumption of yield lines under the united action of bending moment and membrane force is:

$$J_{mn} = \sum_i \int_{l_i} \dot{D}_i dl \tag{7}$$

in which l_i is the length of yield line NO. *i*. On the other hand, when only bending moments acted on, the power consumption is:

$$J_m = M_0 \sum_i \dot{\theta}_i l_i \tag{8}$$

Based on the energy dissipation principle, the corrected parameter is defined to characterize membrane force effect by the ratio of the power consumptions:

$$f_n = \frac{J_{mn}}{J_m} \tag{9}$$

By introducing membrane force factor, namely replacing M_0 by $f_n M_0$,the motion equations of large deformation for failure mode B can be obtained:

$$\begin{aligned} &\ddot{\phi}_1 \xi^3 (2-3\delta) = p(\tau)(3-4\delta)\xi^2 - 6\alpha f_n \\ &\ddot{\phi}_2 \delta^3 (2-3\xi) = p(\tau)(3-4\xi)\delta^2 - 6\gamma^2 \alpha f_n \\ &\frac{d}{d\tau}\left(\dot{\phi}_1 \xi\right) = p(\tau) \\ &\dot{\phi}_1 \xi = \dot{\phi}_2 \delta \end{aligned} \tag{10}$$

in which, τ is dimensionless moment ($\tau = t\sqrt{M_0/\mu H b^2}$); $\phi_1 = \overline{\phi}_1 \, \mathrm{b/H}, \phi_2 = \overline{\phi}_2 \, \mathrm{a/H}, \overline{\phi}_1, \overline{\phi}_2$ is rotation angle around boundary of rigid block ① and ②; $p(\tau) = p(t)b^2/M_0$.

When δ=1/2, the corresponding motion equations for failure mode A can be derived.

For Eq. (10) is ordinary differential equations about $\xi(\tau), \delta(\tau), \dot{\phi}_1(\tau)$ and $\dot{\phi}_2(\tau)$, the relative differential equations can be obtained:

$$\xi\ddot{\xi} I(\tau)(2-3\delta) + (1-\delta)\xi^2 p(\tau) = 6\alpha \,, \quad \delta\ddot{\delta} I(\tau)(2-3\xi) + (1-\xi)\delta^2 p(\tau) = 6\gamma^2\alpha \tag{11}$$

By substituting $\tau = 0$, and combining static limit equilibrium Eq. (2-B) and Eq. (10), the critical load is brought about:

$$p^*\left(1-\delta_0\right)\xi_0{}^2 / p_0 = \xi_p^2, \quad 4p^*\left(1-\xi_0\right)\delta_0{}^2 / p_0 = 3-4\xi_p \tag{12}$$

Define critical parameters $\zeta = p^*/p_0$. For $p^* > p_0$, $1 < \zeta < \infty$. The critical load of failure mode A and B can be obtained by insetting $\delta_0 = 1/2$ into Eq.(12):

$$\zeta_{cr} = (3-4\xi_p+\xi_p{}^2)+\sqrt{2\xi_p{}^2(3-4\xi_p)+\xi_p{}^2} \tag{13}$$

If $p \le \zeta_{cr} p_0$, only model A will come up with no plastic flat area during the whole response process. When $\gamma = 1$, $\zeta_{cr} \to 2$; When $\zeta_{cr} \to 2$, $\zeta_{cr} \to 3$.

4 DYNAMIC RESPONSE OF A CLAMPED RECTANGULAR PLATE UNDER EXPLOSION LOAD

If the peak pressure is less than limit load p_0, the plate will be at rigid state. Here the plastic deformation of the rectangular plate is analyzed by applying the secondary explosion load ($p_0 \le p_m \le \zeta_{cr} p_0$) and higher load ($p_m > \zeta_{cr} p_0$).

Considering the hysteresis of material motion, it is more practical to divide the motion modes according to deflection. The deflection limits should be defined as $\eta = 1/5$ based on classical small deformation theory of thin plate. Here η is the ratio of the deflection ω_0 in the center and thickness H :

$$\eta = \frac{\omega_0}{H} = \frac{1}{H}\int_0^\tau b\xi \frac{d\overline{\phi_1}}{dt} dt = \int_0^\tau \xi \dot{\phi}_1 d\tau \tag{14}$$

4.1 The movement patterns of rectangular plate under secondary load

Small deformation of mode A comes up firstly under secondary load ($p_0 \le p_m \le \zeta_{cr} p_0$), namely $\delta_0 = 1/2$. The stage of $p < p_0$ can be ignored because of short duration. The initial moment t_0 of the deformation can be obtained by $p(\tau_0) = p_0$. Motion equations during this stage can be obtained:

$$\begin{aligned} &\ddot{\phi}_{11}\xi^3 = 2p(\tau)\xi^2 - 24 \\ &\ddot{\phi}_{21}(2-3\xi) = 2p(\tau)(3-4\xi) - 48\gamma^2 \\ &2\dot{\phi}_{11}\xi = \dot{\phi}_{21}(\textit{continuity condition}) \end{aligned} \tag{15}$$

Based on the angular velocity $\dot{\phi}_1 = \dot{\eta}/\xi$ of rigid piece around boundary, the deflection can be derived by $\eta_1 = \int_{\tau_0}^{\tau} \xi_1(\tau)\dot{\phi}_{11} d\tau$. By insetting $\eta_1 = 1/5$, the critical time t_1 when large deformation is reached can be calculated.

4.1.1Motion model Ⅰ

$t_1 \le t_s$ means that large deformation has been reached before the explosion load ends, as shown in Fig. 2.

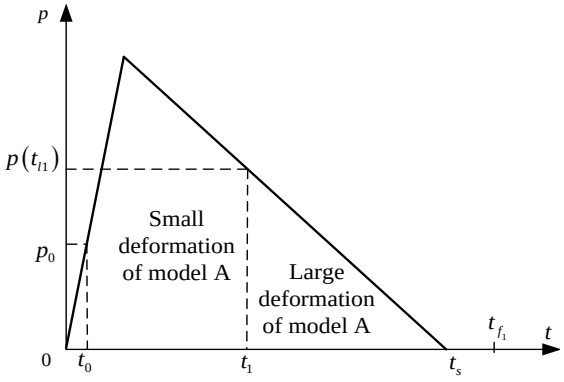

Fig.2 Time history of motion model (1-A)

During $t_1 < t \le t_s$, the motion equations of plate are:

$$\ddot{\phi}_{12}\xi^3 = 2p(\tau)\xi^2 - 24f_1;\ \ \ddot{\phi}_{22}(2-3\xi) = 2p(\tau)(3-4\xi) - 96\gamma^2 f_2;\ \ 2\dot{\phi}_{12}\xi = \dot{\phi}_{22} \tag{16}$$

When $t > t_s$, the action of load is over. Until the development of yield line stops, the motion equations are:

$$\ddot{\phi}_{13}\xi^3 = -24f_1;\ \ \ddot{\phi}_{23}(2-3\xi) = -96\gamma^2 f_2;\ \ \ 2\dot{\phi}_{13}\xi = \dot{\phi}_{23} \tag{17}$$

To determine the moment τ_{f1} when the motion stops, inset $\dot{\xi}_3(\tau_{f1}) = 0$. The final deflection can be obtained:

$$\eta_3 = \int_{\tau_0}^{\tau_1} \xi_1(\tau)\dot{\phi}_{11}d\tau + \int_{\tau_1}^{\tau_s} \xi_2(\tau)\dot{\phi}_{12}d\tau + + \int_{\tau_s}^{\tau_f} \xi_3(\tau)\dot{\phi}_{13}d\tau \tag{18}$$

4.1.2 Motion model Ⅱ

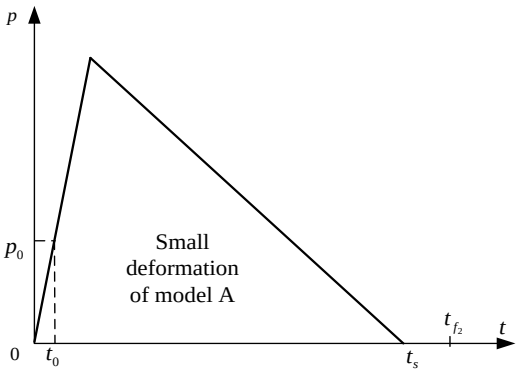

Fig.3 Time history of motion model (2-A)

$t_1 \geq t_s$ means that the small deflection continues during and after the explosion load acted on, as shown in Fig. 3.

After the load acted on, the motion equations of plate are expressed with that of small deflection:

$$\ddot{\phi}_{14}\xi^3 = -24; \quad \ddot{\phi}_{24}(2-3\xi) = -48\gamma^2; \quad 2\dot{\phi}_{14}\xi = \dot{\phi}_{24} \tag{19}$$

According to $\dot{\xi}_4 = 0$, the ending moment τ_{f2} can be derived. The final deflection is:

$$\eta_4 = \int_{\tau_0}^{\tau_s} \xi_1(\tau)\dot{\phi}_{11} d\tau + \int_{\tau_s}^{\tau_f} \xi_4(\tau)\dot{\phi}_{14} d\tau \tag{20}$$

4.2The movement patterns of rectangular plate under high load

Under high load($p_m > \zeta_{cr} p_0$), the failure mode B comes up at first, then returning back to mode A. Regard the stage of $p < \zeta_{cr} p_0$ as rigid state of the plate. By insetting $p(\tau_0^*) = \zeta_{cr} p_0$ into the expression of explosion load, the initial moment t_0^* can be obtained. The motion equations of small deflection after t_0^* are:

$$\begin{aligned} &\ddot{\phi}_{1I}\xi^3(2-3\xi) = p(\tau)(3-4\delta)\xi^2 - 12; \ \ddot{\phi}_{2I}\delta^3(2-3\xi) = p(\tau)(3-4\xi)\delta^2 - 12\gamma^2 \\ &\frac{d}{d\tau}(\dot{\phi}_{1I}\xi) = p(\tau); \quad \dot{\phi}_{1I}\xi = \dot{\phi}_{2I}\delta \end{aligned} \tag{21}$$

Differential equations of the yield line expressions can be derived:

$$\dot{\xi} = \left[12 - (1-\delta)\xi^2 p(\tau)\right] / \left[\xi I(\tau)(2-3\delta)\right], \quad \dot{\delta} = \left[12\gamma^2 - (1-\xi)\delta^2 p(\tau)\right] / \left[\delta I(\tau)(2-3\xi)\right] \tag{22}$$

The initial value of ξ_0, δ_0 can be obtained according to static limit equations, thus deriving $\xi_{\mathrm{I}}(\tau), \delta_{\mathrm{I}}(\tau)$. The deflection at this stage is:

$$\eta_{\mathrm{I}} = \int_{\tau_0^*}^{\tau} \xi_{\mathrm{I}}(\tau)\dot{\phi}_{1\mathrm{I}} d\tau \tag{23}$$

The critical time t_2 when large deformation is reached can be obtained by insetting $\eta_{\mathrm{I}} = 1/5$.

4.2.1Motion model one

$t_2 \geq t_s$ means that there comes no large deformation during the process. Then the moment t_{l1} when the motion transforms from mode B to mode A can be derived by calculating $\delta_{\mathrm{I}}(\tau_{l1}) = 1/2$. Whether the moment is before or after the acting time t_s contributes to two different situations.

(1) $t_{l1} < t_s$, which means the transforming moment is ahead of the acting load ending, the

time-history is as shown in Fig. 4.

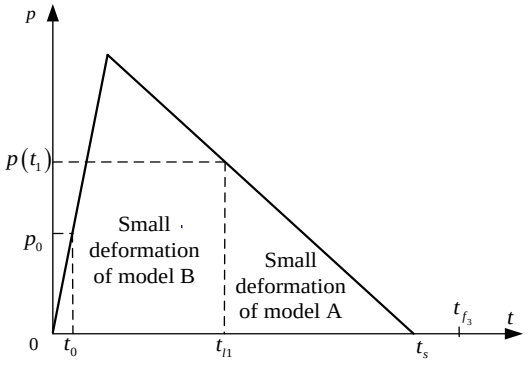

Fig.4 Time history of motion model (1-B)

During $t_{l1} < t \le t_s$, the motion equations can be expressed as:

$$\ddot{\phi}_{1\text{II}}\xi^3 = 2p(\tau)\xi^2 - 24;\ \ddot{\phi}_{2\text{II}}(2-3\xi) = 2p(\tau)(3-4\xi) - 48\gamma^2;\ \ 2\dot{\phi}_{1\text{II}}\xi = \dot{\phi}_{2\text{II}} \tag{24}$$

When $t > t_s$, small deformation of mode A continues, of which the motion equations are:

$$\ddot{\phi}_{1\text{III}}\xi^3 = -24;\ddot{\phi}_{2\text{III}}(2-3\xi) = -48\gamma^2;2\dot{\phi}_{1\text{III}}\xi = \dot{\phi}_{2\text{III}} \tag{25}$$

When the motion of plate stops, meaning of $\dot{\xi}_{\text{III}} = 0$, the finish moment t_{f3} can be derived. The final deflection is:

$$\eta_{\text{III}} = \int_{\tau_0}^{\tau_{l1}} \xi_{\text{I}}(\tau)\dot{\phi}_{1\text{II}}d\tau + \int_{\tau_{l1}}^{\tau_s} \xi_{\text{II}}(\tau)\dot{\phi}_{1\text{III}}d\tau + \int_{\tau_s}^{\tau_{f3}} \xi_{\text{III}}(\tau)\dot{\phi}_{1\text{III}}d\tau \tag{26}$$

(2)If $t_{l1} \ge t_s$, which small deformation of mode B continues during and after the explosion load acted on, the time-history is as shown in Fig. 5.

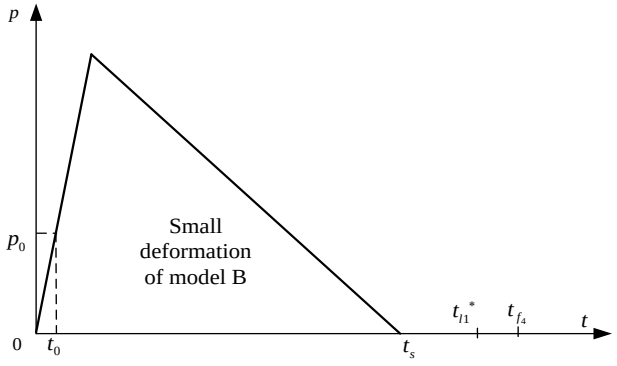

Fig.5 Time history of motion model (2-B)

After load acted on, $t_s < t \le t_{l1}^*$, small deformation of mode B develops until $\delta = 1/2$. The motion equations are:

$$\ddot{\phi}_{1\text{II}^*}\xi^3(2-3\xi) = -12; \quad \ddot{\phi}_{2\text{II}^*}\delta^3(2-3\xi) = -12\gamma^2; \quad \dot{\phi}_{1\text{II}^*}\xi = \dot{\phi}_{2\text{II}^*}\delta \tag{27}$$

By insetting $\delta = 1/2$, the moment t_{l1}^* when the deformation of plate transforms from mode B to mode A can be obtained by $\delta_{\text{II}^*}(\tau_{l1}^*)$.

When $t > t_{l1}^*$, it comes to be small deformation of mode A, and the motion equations are:

$$\ddot{\phi}_{1\text{III}^*}\xi^3 = -24; \quad \ddot{\phi}_{2\text{III}^*}(2-3\xi) = -48\gamma^2; \quad 2\dot{\phi}_{1\text{III}^*}\xi = \dot{\phi}_{2\text{III}^*} \tag{28}$$

The moment τ_{f4}, when the motion of plate stops, can be derived by assuming $\dot{\xi}_{\text{III}^*} = 0$. Then the final deflection is:

$$\eta_{\text{III}^*} = \int_{\tau_0}^{\tau_s} \xi_{\text{I}}(\tau)\dot{\phi}_{1\text{I}}d\tau + \int_{\tau_s}^{\tau_{l1}^*} \xi_{\text{II}^*}(\tau)\dot{\phi}_{1\text{III}^*}d\tau + \int_{\tau_{l1}^*}^{\tau_{f4}} \xi_{\text{III}^*}(\tau)\dot{\phi}_{1\text{III}^*}d\tau \tag{29}$$

4.2.2Motion model two

$t_2 < t_s$ means that the large deformation sets out before the acting load ends.

During $t_2 \le t < t_s$, the motion equations within membrane force factor employed are:

$$\begin{aligned} &\ddot{\phi}_{1\text{IV}}\xi^3(2-3\delta) = p(\tau)(3-4\delta)\xi^2 - 12f_1 \\ &\ddot{\phi}_{2\text{IV}}\delta^3(2-3\xi) = p(\tau)(3-4\xi)\delta^2 - 12\gamma^2 f_2 \\ &\frac{d}{d\tau}(\dot{\phi}_{1\text{IV}}\xi) = p(\tau); \quad \dot{\phi}_{1\text{IV}}\xi = \dot{\phi}_{2\text{IV}}\delta \end{aligned} \tag{30}$$

Until when the deformation of the plate transforms from mode B to mode A, the moment t_{l2} can be determined by assuming $\delta = 1/2$.

(1)If $t_{l2} \le t_s$, the transformation moment of mode B and mode A is ahead of the load ends, and the time-history is as shown in Fig. 6.

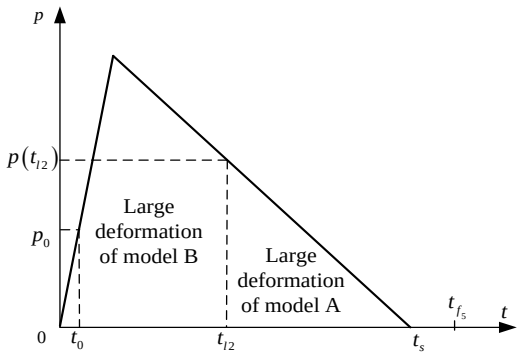

Fig.6 Time history of motion model (1-B)

During $t_{l2} \le t < t_s$, the motions equations of large deformation with mode A applied are:

$$\begin{aligned} &\ddot{\phi}_{1} \xi^3 = 2p(\tau) - 24 f_1 \\ &\ddot{\phi}_{2} (2-3\xi) = 2p(\tau)(-3\xi) + 96\gamma^2 f_2 \quad \dot{\phi}_1 \xi = \dot{\phi}_2 \end{aligned} \tag{31}$$

When $t \ge t_s$, the large deformation with mode A continues and the motion equations are:

$$\ddot{\phi}_{1\mathrm{VI}} \xi^3 = -24 f_1; \quad \ddot{\phi}_{2\mathrm{VI}} (2-3\xi) = -96\gamma^2 f_2; \quad 2\dot{\phi}_{1\mathrm{VI}} \xi = \dot{\phi}_{2\mathrm{VI}} \tag{32}$$

When the motion of plate stops at the moment t_{f5}, which can be determined by $\dot{\xi}_{\mathrm{VI}}(\tau_{f5}) = 0$, the final deflection can be calculated:

$$\eta_{\mathrm{VI}} = \eta_{\mathrm{V}} + \int_{\tau_s}^{\tau_{f5}} \xi_{\mathrm{VI}}(\tau)\dot{\phi}_{1\mathrm{VI}} d\tau = \int_{\tau_0^*}^{\tau_{l2}} \xi_{\mathrm{I}}(\tau)\dot{\phi}_{1\mathrm{II}} d\tau + \int_{\tau_{l2}}^{\tau_s} \xi_{\mathrm{V}}(\tau)\dot{\phi}_{1\mathrm{V}} d\tau + \int_{\tau_s}^{\tau_{f5}} \xi_{\mathrm{VI}}(\tau)\dot{\phi}_{1\mathrm{VI}} d\tau \tag{33}$$

(2)If $t_{l2} > t_s$, the large deformation with mode B continues during the load acting on, as shown in Fig. 7.

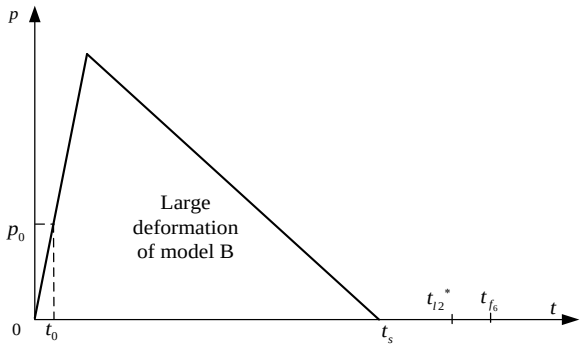

Fig.7 Time history of motion model (2-B)

When $t_s < t \le t_{l2}^*$, the motion equations of plate are:

$$\ddot{\phi}_{1\mathrm{V}^*} \xi^3 (2-3\delta) = -12 f_1; \quad \ddot{\phi}_{2\mathrm{V}^*} \delta^3 (2-3\xi) = -12\gamma^2 f_2; \quad \dot{\phi}_{1\mathrm{V}^*} \xi = \dot{\phi}_{2\mathrm{V}^*} \delta \tag{34}$$

By assuming $\delta = 1/2$, the transforming moment t_{l2}^* can be determined.

When $t_{l2}^* < t \le t_{f6}$, large deformation with mode A comes up, of which the motion equations are:

$$\ddot{\phi}_{1\mathrm{VI}^*} \xi^3 = -24 f_1; \quad \ddot{\phi}_{2\mathrm{VI}^*} (2-3\xi) = -96\gamma^2 f_2; \quad 2\dot{\phi}_{1\mathrm{VI}^*} \xi = \dot{\phi}_{2\mathrm{VI}^*} \tag{35}$$

When the motion of the plate stops at the moment t_{f6}, which can be determined by $\dot{\xi}_{\mathrm{VI}^*}=0$, the final deflection can be obtained:

$$\eta_{\mathrm{VI}^*}=\int_{\tau_0}^{\tau_2}\xi_{\mathrm{I}}(\tau)\dot{\phi}_{1\mathrm{I}}(\tau)d\tau+\int_{\tau_2}^{\tau_s}\xi_{\mathrm{IV}}(\tau)\dot{\phi}_{1\mathrm{IV}}(\tau)d\tau+\int_{\tau_s}^{\tau_{l2}^*}\xi_{\mathrm{V}^*}(\tau)\dot{\phi}_{1\mathrm{V}^*}(\tau)d\tau+\int_{\tau_{l2}^*}^{\tau_{f6}}\xi_{\mathrm{VI}^*}(\tau)\dot{\phi}_{1\mathrm{VI}^*}(\tau)d\tau \quad (36)$$

During the whole analysis, the moment of plate stops during a certain stage hasn't been checked. So by checking the moment after the expression of yield lines being calculated, the complete deformation process of the plate under explosion load can be obtained.

5 NUMERICAL EXPERIMENTS

5.1The establishment of the numerical model

In a numerical experiment, assume the air as ideal gas, specific heat ratio $\gamma=1.4$, density ρ_0=1.29kg/m^3, and the initial internal energy $E_0=2.5\times10^5 J/m^3$.

For TNT, the initial density ρ_0=1630kg/m^3, initial internal energy of unit volume $E_0=6.0\times10^3$MJ/m^3. JWL model is simulated to explosive in numerical analysis, of which material parameters are determined by test.

With the material model JOHNSON_COOK proposed by Johnson GR, the parameters of concrete (compressive strength 48MPa, density $\rho_0=2440$kg/m^3) was provided[7]. In a similar way, the parameters of concrete (35Mpa, $\rho_0=2550$kg/m^3) can be obtained, as shown in Table 1.

Table 1 The parameters of reinforced concrete(35MPa) in JHC model

RO (kg/m^3)	G (Gpa)	A	B	C	N	f_c' (MP)	T (MPa)	$EPS0$	$EFMIN$
2550	12.78	0.79	1.6	0.007	0.61	35	3.6	1^E-6	0.01
$SFMAX$ (GPa)	P_c (MPa)	μ_{crush}	P_l (GPa)	μ_{lock}	D_1	D_2	K_1 (GPa)	K_2 (GPa)	K_3 (GPa)
700	11.67	6.85^E-4	0.038	0.05	0.0368	1.0	85	-171	208

To take the minimum tensile strain as failure criterion, the strain rate sensitivity should be considered. So the failure stain of concrete in this numerical experiment is 0.001.

5.2 Different failure modes

The reinforced concrete plate, with size of 1000mm×2000mm×100mm, the steel of 8 mm-diameter and 235 MPa -yield stress, is taken as objects. By the layout with double-deck and two-way, reinforcement distribution modes of long side is 100mm×10 and that of short side is120mm×17.

Explosion of different charge(0.81kg、1.25kg、1.82kg and 2.50kg)is employed to act on the reinforced concrete slab, which is simply supported, and the explosive distance is 0.5m.

The time history of displacement in the center of plate is as shown in Fig.8.

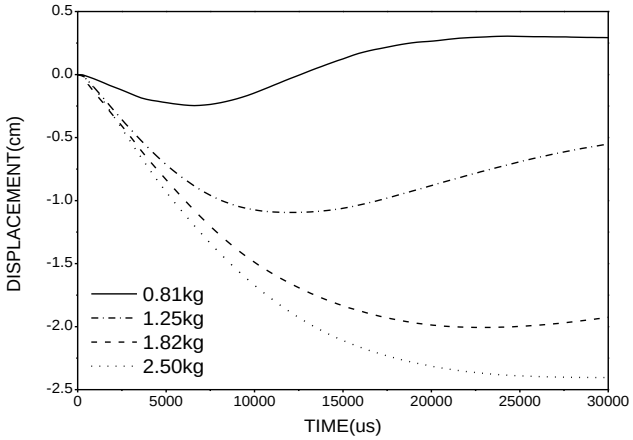

Fig.8 Time history of displacement in the center of plate

Fig.8 tells that, with the explosive charge adding, the displacement of the central region increases gradually, and the whole elastic deformation turns to stable plastic deformation.

The comparison of theoretical analysis results and numerical ones is as Table.2.

Table 2 Comparison between numerical simulation and theoretical analysis

charge(kg) / terms	0.81	1.25	1.82	2.5
Load	Low	Secondary	Secondary	Higher
Motion mode	----	SEC-2	SEC-1	HIG-1-B
Theoretical displacement(mm)	----	30.55	79.51	74.46
Numerical displacement(mm)	2.50	10.20	20.10	23.20

As shown in Table.2, the results of theoretical calculation are bigger than the numerical ones in general. This is because of the ignorance of the strengthening effects of materials etc. in theoretical analysis. So the numerical study which took these effects into account is more approximate with the practical. But the similar tendency and results confirm the efficiency of the theory discussed in this paper.

6 CONCLUSION

Theoretical analysis and numerical simulation are both employed to analyze the dynamic response of reinforced concrete rectangular plate under explosive load in this paper. The

theory performed in this paper is proved efficient and available with the comparison of theoretical results and numerical ones. The main conclusions are:

(1)According to the energy method and the plastic hinge line theory, the effect of the membrane force on neutral plane applied on plate with large deformation is taken into account. The membrane force factor is introduced into the motion equations.

(2)When under secondary and higher explosion load, the motion and deformation of the plate are analyzed with the two different failure modes and corresponding motion equations. And the whole process of the deformation is received by numerical calculation.[i]

REFERENCES

[1] Josef Henrych. Dynamics of explosion and its use[J]. *Elsevier Scientific Pub. Co.* 1979:212-278

[2] Xiao Chaoxiong. Research on the ultimate strength and bending rigidity of minor axis T-sub semi-rigid connections[D]. *Master Degree Thesis of Hunan University,* 2009: 12-14

[3] Zhu Wei. Dynamic Plastic Response of Stiffened Plates Subjected to Explosive Impact Loading[D]. *Master Degree Thesis of Huazhong University of Science and Technology,* 2012: 23-26

[4] Chen Faliang, Yu Tongxi. Dynamic plastic response of rectangular plates with plastic energy dissipation[J]. *Explosion and Shock Waves,* 2005,25(3):200-206

[5] Yu Tongxi, Qiu Xinming. impact dynamics[D]. *Tsinghua University press,* 2011: 112-124

[6] Jones N. A theoretical study of the dynamic plastic behavior of beams and plates with finite deflections[J]. *Inter-national Journal of Solids & Structures,* 1971(7): 1007 -1029.

[7] Johnson GR，Cook WH. A constitutive model and data for metals subjected to large strain, high strain rates and high temperatures. *Proceedings of the 7th international symposium on ballistics*，The Hague：541-547

[i] This paper is funded by the international Exchange Program of Harbin Engineering University for Innovation-oriented Talents Cultivation.

The paper is supported financially by the Fundamental Research Funds for the Central Universities (HEUCF130214).